

# Universal Person Re-Identification

**Xu Lan**

Queen Mary University of London  
x.lan@qmul.ac.uk

**Xiatian Zhu**

Vision Semantics Ltd.  
eddy.zhuxt@gmail.com

**Shaogang Gong**

Queen Mary University of London  
s.gong@qmul.ac.uk



Figure 1: Universal person appearance transformations for training a single domain-generic re-id model enabling universal deployments. Compared to existing methods typically focusing on domain-specific model training (“train once, run once”), the proposed method allows for a “train once, run everywhere” pattern therefore favourably suits the industrial scale large system development without the need of training the system to every individual target domain as prior of each deployment.

## Abstract

Most state-of-the-art person re-identification (re-id) methods depend on supervised model learning with a large set of cross-view identity labelled training data. Even worse, such trained models are limited to only the same-domain deployment with significantly degraded cross-domain generalisation capability, i.e. “*domain specific*”. To solve this limitation, there are a number of recent unsupervised domain adaptation and unsupervised learning methods that leverage unlabelled target domain training data. However, these methods need to train a separate model for each target domain as supervised learning methods. This conventional “*train once, run once*” pattern is unscalable to a large number of target domains typically encountered in real-world deployments. We address this problem by presenting a “*train once, run everywhere*” pattern industry-scale systems are desperate for. We formulate a “*universal model learning*” approach enabling domain-generic person re-id using only limited training data of a “*single*” seed domain. Specifically, we train a universal re-id deep model to discriminate between a set of transformed person identity classes. Each of such classes is formed by applying a variety of random appearance transformations to the images of that class, where the transformations simulate the camera viewing conditions of any domains for making the model train-

ing domain generic. Extensive evaluations show the superiority of our method for universal person re-id over a wide variety of state-of-the-art unsupervised domain adaptation and unsupervised learning re-id methods on five standard benchmarks: Market-1501, DukeMTMC, CUHK03, MSMT17, and VIPeR.

## Introduction

The aim of person re-identification (re-id) is to recognise the fine-grained person identity information in detected bounding boxes captured from non-overlapping surveillance camera views (Gong et al. 2014). State-of-the-art re-id methods train deep Convolutional Neural Network (CNN) models in a *supervised learning* manner and dramatically improve the matching performance (Sun et al. 2018; Li, Zhu, and Gong 2018; Zhang et al. 2018; Li, Zhu, and Gong 2017; Wei et al. 2017; Wang et al. 2018a; Xu et al. 2018; Song et al. 2018). Supervised model learning often assumes *only* the same-domain (i.e. surveillance camera network) deployment with drastic performance drop for new unseen domains, as the model is trained specifically to well fit a large training



Figure 2: Four representative model learning strategies for person re-id: (a) *Supervised model learning* on a large set of cross-camera identity labelled training data per domain. Once trained, the model is deployed for the same domain alone. (b) *Unsupervised domain adaptation* on labelled training data from a source domain and unlabelled training data from the target domain. The adapted model is specific for the target domain. (c) *Unsupervised model learning* on unlabelled training data of the target domain. The trained model is specific for the target domain. (d) *Universal model learning* on labelled training samples from a seed domain. Once trained the model can be *frozen forever* and applied for universal person re-id deployment at any target domains including the seed domain.

set per domain (Fig. 2(a)). This restricts severely their scalability and deployability in real-world applications where no manually labelled training data is typically available for target domains. Exhaustive cross-camera labelling is rather expensive and not always available, due to a quadratic number of camera view pairs in each surveillance domain.

There are a small number of recent attempts that aim for solving the aforementioned generalisation limitations of supervised learning re-id methods. Their high-level modelling strategies fall generally into three groups: (i) *hand-crafting features* (Farenzena et al. 2010; Cheng et al. 2011; Liao et al. 2015; Zheng et al. 2015), (ii) *unsupervised domain adaptation* (Peng et al. 2016; Zheng et al. 2017; Deng et al. 2018; Wang et al. 2018b; Lin et al. 2018; Zhong et al. 2018; Yu et al. 2019), (iii) *unsupervised deep learning* (Chen, Zhu, and Gong 2018; Lin et al. 2019; Li et al. 2018). Hand-crafting feature representations are largely domain generic and universal without the need for training. However, they suffer from much inferior re-id performances than the latter two approaches, due to rather limited appearance knowledge involved. Whilst significant performance gains have been achieved on unlabelled target domains, existing unsupervised domain adaptation (Fig. 2(b))

and unsupervised model learning (Fig. 2(c)), often take a “*train once, run once*” pattern. That is, a trained model by them is effective only for the target domain that the model training is applied to. For every single target domain deployment, a new model needs to be trained through the same optimisation process repeatedly. Such a *domain-specific* property reduces their practical value and limits their scalability significantly, considering potentially a very large quantity of different domains to be targeted in real-world applications.

In this work, we consider a “*train once, run everywhere*” pattern. In contrast to all the existing methods, we train a re-id model using the labelled data from a single *seed* domain, and *frozen* it for universal deployment at any domains *without* further training and/or fine-tuning the model to any target domains (Fig. 2(d)). To this end, we propose a *Universal Model Learning* (UML) method capable of training a *single* model for domain generic person re-id deployment. UML trains a universally deployable re-id model *one-off* on transformed seed training data, without the need of using any target domain data for model learning and refinement. The image transformations are designed to produce an extremely rich and diverse training dataset (Fig. 1) that simulates camera viewing condition variations as completely as possible for different domains, i.e. *domain complete therefore domain generic*. The viewing condition variations are simulated by randomly applying fundamental colour and contrast transformations to a labelled seed person image. This image and its transformed versions share the same identity label. By design, the re-id model trained on the proposed augmented dataset is discriminative and effective universally for any domains.

Our *contributions* of this work are summarised as follows: (1) We present a “*train once, run everywhere*” pattern for universal person re-identification. This differs dramatically from the conventional state-of-the-art re-id methods in form of “*train once, run once*”, which is unsuitable and unscalable for practical large scale system development and deployment in industrial applications. To our knowledge, this is the first deep learning attempt of universal person re-id. (2) We propose a simple yet effective *Universal Model Learning* (UML) approach for realising universal person re-id. UML is based on comprehensive and rich image transformations in colour and contrast given a labelled seed training dataset. This image generation method is computationally efficient, flexible in design, and domain generic, without the need for complicated image synthesis model design and intricate hyper-parameter tuning per domain as required by state-of-the-art methods. (3) We summarise the existing methods of unsupervised domain adaptation and unsupervised learning applicable for person re-id in unlabelled target domains, and compare them with the proposed UML method in proper perspective. Extensive evaluations demonstrate the model training and performance superiority of our method over the state-of-the-art alternative methods on five person re-id benchmarks: Market-1501, DukeMTMC-reID, CUHK03, MSMT17, and VIPeR.

## Related Work

**Supervised person re-id.** In the literature, existing person re-id methods mostly focus on *supervised model learning* (Gong et al. 2014; Li et al. 2014; Zheng et al. 2015; Li, Zhu, and Gong 2017; Chen, Zhu, and Gong 2018; 2017; Wang et al. 2014; Xiao et al. 2016; Wang et al. 2018a; Li, Zhu, and Gong 2018; Chang, Hospedales, and Xiang 2018; Sun et al. 2018; Chen et al. 2017; Yu et al. 2018; Shen et al. 2018; Xu et al. 2018; Wang et al. ). This type of methods requires to access a large set of cross-camera identity labelled training samples acquired through an exhaustive and costly annotation process. Deploying a pre-trained re-id model to unseen new domains often encounter dramatic performance drops. Due to this prerequisite for model supervised optimisation, their scalability and usability are dramatically restricted in real-world applications. This is because, we often have no access to any cross-camera identity labelled training data for target deployment domains in practical use. Earlier hand-crafted features based models (Farenzena et al. 2010; Cheng et al. 2011; Liao et al. 2015; Zheng et al. 2015; Zhao, Oyang, and Wang 2017) are domain generic, but yield significantly inferior model performance.

**Unsupervised domain adaptation person re-id.** The limitation of supervised learning re-id methods in cross-domain scalability can be addressed by using unsupervised domain adaptation (UDA) techniques. Existing UDA re-id methods generally fall into two categories: (1) image synthesis (Deng et al. 2018; Zhong et al. 2018; Bak et al. 2018; Qian et al. 2018), and (2) feature alignment (Peng et al. 2016; Yu et al. 2019; Yu, Wu, and Zheng 2017; Wang et al. 2018b; Lin et al. 2018). The former aims to transfer the labelled source identity classes from the source domain to the target domain through cross-domain conditional image generation in the appearance style and background context at pixel level. The synthetic images are then used to fine-tune the model towards the target domain. On the contrary, the latter transfers the discriminative feature information learned from the labelled source training data to the target feature space by distribution alignment. These methods often use discrete attribute labels for facilitating the information transition across domains due to their better domain invariance property than low-level feature representations.

**Unsupervised learning person re-id.** In parallel to UDA re-id methods, unsupervised learning methods have started to gain increasing potentials for eliminating the need of labelling large training data (Kodirov et al. 2015; Lisanti et al. ; Li et al. 2018; Lin et al. 2019; Chen, Zhu, and Gong 2018). Such methods rely on the reconstruction loss designs (Kodirov et al. 2015; Lisanti et al. ) or self-discovered cross camera label information by the in-training model for self-supervised learning (Li et al. 2018; Lin et al. 2019; Chen, Zhu, and Gong 2018). The methods assume access of unlabelled training data sampled from the target domain, and train a domain-specific re-id model.

**Universal learning person re-id.** In this work, we present universal learning person re-id, which differs dramatically

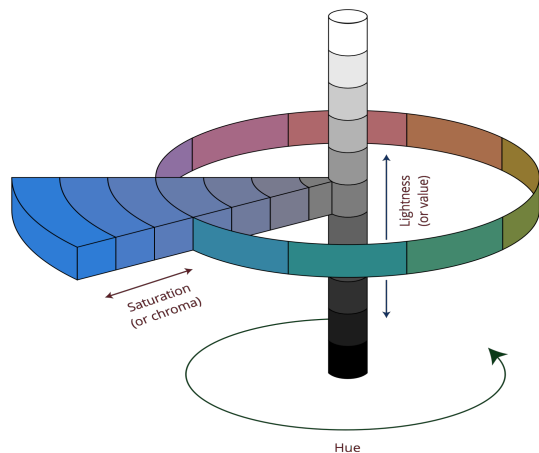


Figure 3: Illustration of Munsell colour system in three dimensions: Hue, Saturation, Lightness. This graph is adopted from (Mun ). Best viewed in colour.

from all the existing methods as discussed above. Our method trains a single *domain-generic* re-id model for universal deployments. This is in contrast to previous learning algorithms usually producing *domain-specific* models using either labelled source and/or unlabelled target domain training data. That being said, a separate model training is required for each target domain deployment which is neither cost-effective and convenient nor allowed always for industrial settings. The re-id model trained by our method can be immediately deployed to any domains where no any video and image data are observed to model optimisation. Such universal deployment property is favourable and desired to practical system development. Moreover, the proposed image transformation method is computationally efficient with flexible design due to no need for complex model formulation and costly pixel synthesis model training. In comparison to hand-crafted features (Gray and Tao 2008; Farenzena et al. 2010; Liao et al. 2015; Cheng et al. 2011; Zheng et al. 2015), our model has extra capability for feature representation learning and model optimisation as supervised and unsupervised learning counterparts, whilst simultaneously retaining the merits of domain universality as hand-crafted features. Besides, our learning method differs from and is more scalable than multi-target domain adaptation (Yu, Hu, and Chen 2018; Gholami et al. 2018) where all the target domains need to be observed to training. Conceptually, our method generalises the notion of multi-target domain simultaneous adaptation since we make a model effective for all different domains even without accessing any target domain data.

## Methodology

### Universal Image Transformation

To train a universal person re-id network model, we assume a labelled seed training dataset (i.e. a seed domain)  $\mathcal{I} = \{\mathbf{I}_i, y_i\}_{i=1}^N$ , consisting of  $N$  person bounding box im-

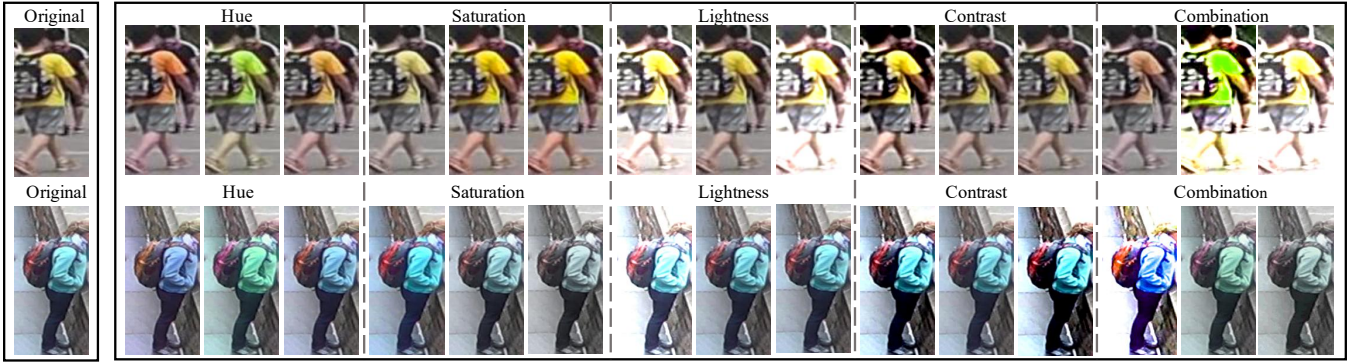


Figure 4: Example transformations in Hue, Saturation (Chroma), Lightness (Value), Contrast, and their random combinations.

ages  $I_i$  each annotated with a person identity class label  $y_i \in \{1, \dots, N_{\text{id}}\}$ . It contains a total of  $N_{\text{id}}$  different person identities.

We propose to transform this seed training set  $D$  so as to cover the camera viewing conditions of arbitrary domains. Formally, we define a set of transformations  $\{\mathcal{M}_t\}$ ,  $t \in \mathcal{T}$  where  $t$  defines the transformation parameter vector and  $\mathcal{T}$  the transformation space. Each transformation  $\mathcal{M}_t$  is composed of several primitive transformations. Consider the variations of person appearance at typical surveillance scenes are largely due to illumination (lighting), we establish a space of linear transformations with regard to pixel colour and contrast. We note that the approach is flexible to adopt other transformations in order to better serve other target domains.

Specifically, we consider the colour transformations in the HSV representation space (Munsell 1919). Each colour has three fundamental attributes (Fig. 3):

1. *Hue*: Colour such as red, orange, yellow, and so forth. It depends on the wavelength of light reflected and/or produced.
2. *Saturation (Chroma)*: The brilliance of a hue, i.e. how pure (intense) a hue is. More saturated a hue is, brighter it appears.
3. *Lightness (Value)*: The lightness or darkness of a hue. Adding white (black) makes the colour lighter (darker). Note, the effect of lightness is relative to other values in a composition.

Specifically, for hue transformation we convert the image into HSV and add the corresponding parameter to the original value on the hue dimension. Afterwards, the image is converted back. For the other factors (including contrast), we perform the transformation by linear interpolation and extrapolation (Haerberli and Voorhies 1994). For restricting the transformations to perceptually sensible scope, we define the variation range as: hue in  $[-18, 18]$  (cyclical), saturation in  $[0.6, 1.4]$ , lightness in  $[0.6, 1.4]$ , and contrast  $[0.6, 1.4]$ . For saturation/lightness/contrast, the value of “1” means *no* transformation, and for hue “0” means *no* transformation.

To form a single colour-contrast transformation, we sample a parameter value for each factor and concatenate them

into a vector  $t$ . We consider an online image transformation strategy for stochastic deep learning. This avoids the need for saving and managing a large quantity of transformed images. In a training iteration, given a seed image  $I_i$ , we sample a randomly parameter vector  $t_i$  and apply the corresponding transformation  $\mathcal{M}_{t_i}$  to it. As such, we obtain a transformed variant:

$$D_i = I_i \mathcal{M}_{t_i}. \quad (1)$$

By repeating the transformation on each and every person image of a training mini-batch, we form domain generic universal training samples  $\{D_i\}$  for model training on-the-fly. We show examples of transformed person images in Fig 4. Perceptually, such transformations leave the original identity class information of person images intact, facilitating the re-id discriminative model optimisation.

### Person Re-Identification Model

For person re-id model, we use ResNet-50 (He et al. 2016) as the backbone network. Other networks (Chang, Hospedales, and Xiang 2018; Li, Zhu, and Gong 2018; Zhang et al. 2018) can be readily considered without any restriction. To enable fine-grained part-level discriminative learning, we adopt the PCB design (Sun et al. 2018). Instead of the whole image, PCB uses average pooling on local regions and applies a separate re-id loss supervision on each individual region independently and concurrently. In addition, we add a parallel global branch for discriminative learning of the whole images. We apply label smoothing for mitigating model overfitting (?). For model training, we adopt the softmax Cross Entropy loss as the objective function:

$$\mathcal{L}_{\text{ce}} = - \sum_{k=1}^{N_{\text{id}}} \sum_{j=1}^m \delta_{k,y} \log(p_j(k|I_i)) + \log(p(k|I_i)) \quad (2)$$

where  $\delta_{k,y}$  is the Dirac delta returning 1 if  $k$  is the ground-truth class label  $y$ , otherwise 0.  $p_j$  and  $p$  denotes the class posterior probability of the  $j$ -th local region and the whole image, estimated by the current network.  $m$  indicates the total number of local regions. We set  $m = 6$  in our experiments the same as (Sun et al. 2018).

Dataset	Train		Test	
	# ID	# Image	# ID	# Image
VIPeR (Gray and Tao 2008)	316	632	316	632
CUHK03 (Li et al. 2014)	767	7,368	700	6,728
Market-1501 (Zheng et al. 2015)	751	12,936	750	19,732
DukeMTMC (Zheng et al. 2017)	702	16,522	702	18,889
MSMT17 (Wei et al. 2018)	1,041	32,621	3,060	93,820

Table 1: Dataset statistics and evaluation setting.

In test, we concatenate all the local regional and global features as the final re-id representation. We adopt the Euclidean distance metric for re-id matching and ranking.

## Remarks

Compared to previous data augmentation approaches (Krizhevsky, Sutskever, and Hinton 2012; Russakovsky et al. 2015), our method differently focuses on training a universal model for any domain generalisation, other than enriching domain-specific training data variety and learning a better model for that domain alone. In particular, we uniquely consider training data transformations that simulate the person appearance distributions and characteristics of arbitrary unseen domains. Such data augmentation is not necessarily beneficial for the labelled training data domain.

As hand-crafted feature representations (Gray and Tao 2008; Farenzena et al. 2010; Cheng et al. 2011; Liao et al. 2015; Zheng et al. 2015), our model learning is universal and domain generic with favourable cross-domain scalability and usability. However, our model is much more discriminative due to the deep model learning capability that is able to learn powerful feature representations. On the contrary, hand-crafted features are based on limited human knowledge which offers significantly weaker discrimination performance.

The closest works to our method are image synthesis based unsupervised domain adaptation re-id models (Bak et al. 2018; Qian et al. 2018; Zhong et al. 2018; Zheng et al. 2017; Deng et al. 2018). All of them aim to transfer the labelled source person identity information to unlabelled target domains. However, these existing methods are domain-specific, and often need a complex model training for every single target domain. This “train once, run once” strategy is less usable and more costly to real-world system development. In contrast, our method needs neither domain-specific training nor difficult model optimisation (such as GANs (Goodfellow et al. 2014)). We take a “train once, run everywhere” strategy based on simple and domain universal image transformations. Our method uses flexibly off-the-shelf supervised learning re-id methods therefore can benefit continuously from a wide range of increasingly advanced learning algorithms developed by the wider community.

## Experiment

**Datasets.** To evaluate our model, we tested five popular person re-id benchmarks. We used the standard train/test eval-

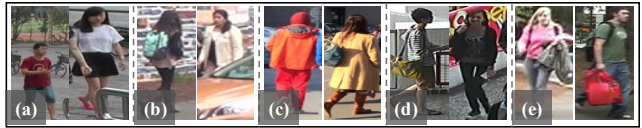


Figure 5: Image examples from the (a) Market-1501, (b) DukeMTMC-reID, (c) MSMT17, (d) CUHK03, and (e) VIPeR person re-id datasets.

uation protocols. The statistics of these datasets are summarised in Table 1. Example person images of these datasets are shown in Fig 5.

**Performance metrics.** We adopted the Cumulative Matching Characteristic (CMC) and mean Average Precision (mAP) as the model performance measurements.

**Implementation details.** We conducted all the experiments in PyTorch (Paszke et al. 2017). To train a universal re-id model, we initialised the model with the parameters pre-trained on ImageNet and used the SGD algorithm with the momentum set to 0.9, the weight decay to 0.0005, and the mini-batch size of 32. We trained the model for totally 60 epochs, with the learning rate of 0.001 in the first 40 epochs, and the decay learning rate as 10 in the last 20 epochs. All input images were resized to  $384 \times 128$  in pixel and subtracted by the ImageNet mean. On top of the proposed transformation strategy, we applied random cropping and flipping during training.

## Universal Learning vs. Unsupervised Learning

We compared our UML model with two hand-crafted feature models, (LOMO (Liao et al. 2015), BoW (Zheng et al. 2015)), two dictionary learning models (ISR (Lisanti et al. ), Dic (Kodirov et al. 2015)), and two unsupervised deep learning methods (TAUDL (Li et al. 2018), BUC (Lin et al. 2019)). In this test, we used MSMT17 and DukeMTMC-reID as the seed training data, individually. Table 2 compares the performance of these methods. We have the following findings.

(1) Hand-crafted feature based re-id methods (Liao et al. 2015; Zheng et al. 2015) produce the weakest matching performance. This is due to poor representation capability of non-learning based features without the ability to extract data relevant feature patterns. Also, these methods cannot optimise the matching metrics.

(2) Dictionary learning based methods (Lisanti et al. ; Kodirov et al. 2015) improve the performance by using reconstruction based learning objective loss functions. However, their capability is limited by the input hand-crafted feature representations.

(3) The more recent unsupervised deep learning models (Li et al. 2018; Lin et al. 2019) further push the performance envelope. In addition to per-domain model training requirement, these methods often come with some extra model parameters which are likely to be data sensitive. Typically, careful parameter tuning and costly model training are re-

Table 2: Universal learning vs. unsupervised learning.

Method	Market-1501				Duke				MSMT17				CUHK03				VIPeR		
	R1	R5	R10	mAP	R1	R5	R10	mAP	R1	R5	R10	mAP	R1	R5	R10	mAP	R1	R5	R10
LOMO (Liao et al. 2015)	27.2	41.6	49.1	8.0	12.3	21.3	26.6	4.8	-	-	-	-	0.6	1.9	3.6	0.7	-	-	-
BOW (Zheng et al. 2015)	35.8	52.4	60.3	14.8	17.1	28.8	34.9	8.3	-	-	-	-	2.1	4.6	7.0	1.9	-	-	-
ISR (Lisanti et al. )	40.3	-	-	14.3	-	-	-	-	-	-	-	-	-	-	-	-	27.0	49.8	61.2
Dic (Kodirov et al. 2015)	50.2	-	-	22.7	-	-	-	-	-	-	-	-	-	-	-	-	29.6	54.8	64.8
TAUDL (Li et al. 2018)	63.7	-	-	<b>41.2</b>	<b>61.7</b>	-	-	<b>43.5</b>	28.4	-	-	12.5	-	-	-	-	-	-	-
BUC (Lin et al. 2019)	66.2	79.6	84.5	38.3	47.4	62.6	68.4	27.5	-	-	-	-	-	-	-	-	-	-	-
<b>UML(MSMT17)</b>	<b>68.2</b>	<b>83.1</b>	<b>87.6</b>	37.0	60.9	<b>83.0</b>	<b>87.5</b>	37.0	-	-	-	-	<b>12.6</b>	<b>25.4</b>	<b>33.4</b>	<b>13.4</b>	<b>36.4</b>	<b>57.9</b>	<b>67.4</b>
<b>UML(Duke)</b>	66.1	81.6	86.3	35.5	-	-	-	-	<b>35.5</b>	<b>48.2</b>	<b>53.7</b>	<b>12.2</b>	10.7	21.9	27.5	10.5	35.4	54.1	62.3
<i>Supervised Learning</i>	90.4	96.5	97.8	73.5	81.5	90.8	93.1	65.9	73.3	84.8	88.1	44.1	40.8	62.7	73.6	40.4	39.2	65.8	77.5

quired in order to achieve competitive results. This is not favourable particularly for unsupervised learning where *no* labelled validation data available for hyper-parameter cross-validation and optimisation for the target domain.

(4) The proposed UML method matches or surpasses the performance of best competitors (Li et al. 2018; Lin et al. 2019) *without* training the model to the target domains. This suggests stronger domain generalisation and practical advantages of our method for the industrial adoption due to the “train once, run everywhere” merit. In reality, model training is costly in both budget and time. This therefore suggests an economical advantages and deployment-friendly superiority of our method over the strongest competitors in practice.

(5) Using MSMT17 as the seed training data leads to slightly better performance as compared to selecting DukeMTMC. This is reasonable since MSMT17 offers more person identities and images.

(6) Compared to supervised learning, both unsupervised and universal learning models are significantly outperformed. This indicates a large room for further algorithm innovation.

### Universal Learning vs. Domain Adaptation

We compared our UML with the state-of-the-art unsupervised domain adaptation re-id methods, including five image synthesis models (PTGAN (Wei et al. 2017), PoseNorm (Qian et al. 2018), SyRI (Bak et al. 2018), SPGAN (Deng et al. 2018), HHL (Zhong et al. 2018)), and six feature alignment models (UMDL (Peng et al. 2016) CAMEL (Yu, Wu, and Zheng 2017), PUL (Fan, Zheng, and Yang 2017), TJ-AIDL (Wang et al. 2018b), MMFA (Lin et al. 2018), DE-CAMEL (Yu et al. 2019)). We make several observations from Table 3 as below.

(1) Feature alignment methods have obtained increasingly higher performance. It is worth noting that most feature learning methods such as DECAMEL unfairly benefit from extra labelled source data.

(2) Compared to feature alignment, image synthesis methods have started to achieve relatively superior cross-domain re-id accuracy. It is especially so considering that less label supervision is used (except SyRI).

(3) UML is the best performer overall among all competitors. Importantly, unlike previous approaches for *domain-specific* model training, our method needs only one time of *domain-generic* model training. This uniquely enables universal person re-id deployments.

(4) Both unsupervised domain adaptation and universal learning are significantly outperformed by the less scalable supervised learning, suggesting the necessity of devoting further more research efforts and endeavour for scaling state-of-the-art re-id methods.

### Further Analysis and Discussions

**Effect of universal image transformations.** We evaluated the performance effect of the proposed universal image transformations. To this end, we compared the results without using our transformations on training data. We tested Market-1501 and DukeMTMC-reID as the seed domain, respectively. Table 4 shows that the proposed image transformation is consistently beneficial for improving the model performance on diverse target domains with very different camera viewing conditions. Both the absolute and relative performance gains are significant in most cases. As we aim for a domain-generic universal person re-id, the performance may be inferior to that of domain-specific models such as supervised learning models. To examine this, we compared UML with the supervised learning model (see the part with grey background). We indeed observe a performance drop but importantly not significant. This means that our model can be similarly effective for the seed domain as the supervised learning method. This differs from most image synthesis adaptation methods which often suffer dramatic performance decrease on the source domain. For example, SPGAN (Deng et al. 2018) experiences a Rank-1 drop of 17.2% (91.6%-74.4%) and 16.4% (83.5%-67.1%) on the source Market-1501 and DukeMTMC-reID, separately.

**Types of image transformations.** We examined the contribution of every individual image transformation: Hue, Saturation, Lightness, and Contrast. Table 5 shows that the performance benefits by individual transformations vary with test domains. This is reasonable due to the difference in the viewing condition characteristics of distinct domains which typically present no regularity. This on the other hand indi-

Table 3: Universal learning vs. unsupervised domain adaptation. \*: Using more labelled source training data. †: Using additionally person attribute labels. UML uses the source data as the seed training samples for fair comparison.

Source→Target	Duke→Market				Market→Duke				CUHK03→Market				CUHK03→Duke			
Metric (%)	R1	R5	R10	mAP	R1	R5	R10	mAP	R1	R5	R10	mAP	R1	R5	R10	mAP
UMDL† (Peng et al. 2016)	34.5	52.6	59.6	12.4	18.5	31.4	37.6	7.3	-	-	-	-	-	-	-	-
PUL (Fan, Zheng, and Yang 2017)	45.5	60.7	66.7	20.5	30.0	43.4	48.5	16.4	41.9	57.3	64.3	18.0	23.0	34.0	39.5	12.0
CAMEL* (Yu, Wu, and Zheng 2017)	54.5	-	-	26.3	-	-	-	-	-	-	-	-	-	-	-	-
TJ-AIDL† (Wang et al. 2018b)	58.2	74.8	81.1	26.5	44.3	59.6	65.0	23.0	-	-	-	-	-	-	-	-
MMFA† (Lin et al. 2018)	56.7	75.0	81.8	27.4	45.3	59.8	66.3	24.7	-	-	-	-	-	-	-	-
DECAMEL* (Yu et al. 2019)	60.2	-	-	32.4	-	-	-	-	-	-	-	-	-	-	-	-
PTGAN (Wei et al. 2017)	38.6	-	66.1	-	27.4	-	50.7	-	31.5	-	60.2	-	17.6	-	38.5	-
PoseNorm (Qian et al. 2018)	-	-	-	-	29.9	-	51.6	15.8	-	-	-	-	-	-	-	-
SPGAN (Deng et al. 2018)	51.5	70.1	76.8	22.8	41.1	56.6	63.0	22.3	42.3	-	-	19.0	-	-	-	-
SyRI* (Bak et al. 2018)	65.7	-	-	-	-	-	-	-	-	-	-	-	-	-	-	-
HHL (Zhong et al. 2018)	62.2	78.8	84.0	31.4	<b>46.9</b>	61.0	66.7	<b>27.2</b>	56.8	74.7	81.4	29.8	42.7	57.5	64.2	23.1
<b>UML(Source)</b>	<b>66.1</b>	<b>81.6</b>	<b>86.3</b>	<b>35.5</b>	46.3	<b>61.2</b>	<b>66.8</b>	26.7	<b>58.7</b>	<b>76.5</b>	<b>82.6</b>	<b>31.1</b>	<b>42.8</b>	<b>57.8</b>	<b>64.3</b>	<b>23.2</b>
<i>Supervised Learning</i>	90.4	96.5	97.8	73.5	81.5	90.8	93.1	65.9	90.4	96.5	97.8	73.5	81.5	90.8	93.1	65.9

Table 4: Effect of universal image transformations (UIT).

Seed	Market				Duke				MSMT17				CUHK03				VIPeR		
	R1	R5	R10	mAP	R1	R5	R10	mAP	R1	R5	R10	mAP	R1	R5	R10	mAP	R1	R5	R10
Market	<b>91.6</b>	<b>97.1</b>	<b>98.0</b>	<b>75.9</b>	40.1	54.9	61.2	23.4	16.0	24.8	29.4	5.0	7.6	15.6	21.1	7.5	29.4	43.4	52.5
<b>Market+UIT</b>	90.4	96.5	97.8	73.5	<b>46.3</b>	<b>61.2</b>	<b>66.8</b>	<b>26.7</b>	<b>24.4</b>	<b>35.7</b>	<b>41.0</b>	<b>7.6</b>	<b>10.0</b>	<b>20.1</b>	<b>26.0</b>	<b>9.9</b>	<b>33.2</b>	<b>48.1</b>	<b>58.2</b>
Gain(absolute)	-1.2	-0.6	-0.2	-2.4	+6.2	+6.3	+5.6	+3.3	+8.4	+10.9	+11.6	+2.6	+2.4	+4.5	+4.9	+2.4	+3.8	+4.7	+5.7
Gain(relative)	-1.3	-0.6	-0.2	-3.2	+15.5	+11.5	+9.2	+14.1	+52.5	+44.0	+39.5	+52.0	+31.6	28.9	+23.2	+32	+12.9	+10.8	+10.9
Duke	57.0	73.9	80.2	30.1	<b>83.5</b>	<b>91.8</b>	<b>94.3</b>	<b>70.0</b>	24.2	34.9	40.3	8.1	8.4	18.2	25.1	8.6	28.2	46.8	57.6
<b>Duke+UIT</b>	<b>66.1</b>	<b>81.6</b>	<b>86.3</b>	<b>35.5</b>	81.5	90.8	93.1	65.9	<b>35.5</b>	<b>48.2</b>	<b>53.7</b>	<b>12.2</b>	<b>10.7</b>	<b>21.9</b>	<b>27.5</b>	<b>10.5</b>	<b>35.4</b>	<b>54.1</b>	<b>62.3</b>
Gain(absolute)	+9.1	+7.7	+6.1	+5.4	-2.0	-1.0	-1.2	-4.1	+11.3	+13.3	+13.4	+4.1	+2.3	+3.7	+2.4	+1.9	+7.2	+7.3	+4.7
Gain(relative)	+16.0	+10.4	+7.6	+17.9	-2.4	-1.1	-1.3	-5.9	+46.7	+38.1	+33.3	+50.6	+27.4	+20.3	+9.6	+22.1	+25.5	+15.6	+8.2

ates the necessity of exploiting all the image transformations for better tackling the domain heterogeneity during deployment at scale.

**Domain universality.** We quantified how well the UML model is generic and universal to various domains in the sense of being robust to transformations. We used the UML model trained with DukeMTMC-reID as the seed domain, and tested its universality degree on transformed Market-1501 images. We selected randomly 1,000 Market-1501 seed (original) images and applied individual transformations to each of them. Compositated transformations were not used for simplified and dedicated analysis. Such transformations imitate the cross-domain person appearance variations. As a comparison, we tested a *baseline* model trained without using our image transformations.

We considered two measures of domain universality: (1) *Feature level invariance*, and (2) *Prediction level invariance*. The former is obtained by computing the Euclidean distance of the features of the transformed images against that of the original images all extracted by the UML model. The latter instead is quantified by the Euclidean distance between their classification prediction vectors. Figure 6 shows that UML enables to learn significantly invariant features w.r.t. image transformations therefore more robust re-id deploy-

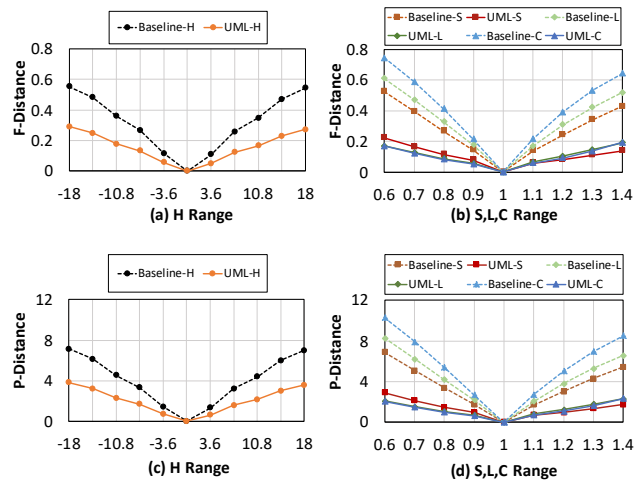


Figure 6: Domain universality analysis. Seed domain: DukeMTMC-reID. Test domain: Market-1501. F=Feature, P=Prediction, H=Hue, S=Saturation, L=Lightness, C=Contrast.

Table 5: Effect of individual image transformations: Hue, Saturation, Lightness, and Contrast.

Seed	Market				Duke				MSMT17				CUHK03				VIPeR		
	R1	R5	R10	mAP	R1	R5	R10	mAP	R1	R5	R10	mAP	R1	R5	R10	mAP	R1	R5	R10
Market	91.6	<b>97.1</b>	<b>98.0</b>	<b>75.9</b>	40.1	54.9	61.2	23.4	16.0	24.8	29.4	5.0	7.6	15.6	21.1	7.5	29.4	43.4	52.5
Market+ <b>H</b>	<b>91.8</b>	96.9	97.8	75.6	41.3	56.6	62.9	23.9	16.3	24.9	29.7	5.1	6.6	14.3	20.0	6.8	29.1	43.4	49.4
Market+ <b>S</b>	91.4	96.8	<b>98.0</b>	75.6	40.4	56.1	62.3	23.5	16.9	25.9	30.8	5.3	7.8	16.8	22.1	7.9	29.4	43.7	53.8
Market+ <b>L</b>	90.9	96.7	<b>98.0</b>	75.1	44.8	59.5	65.1	26.5	18.9	28.6	33.5	5.9	8.4	17.6	22.9	8.4	<b>34.2</b>	47.2	55.4
Market+ <b>C</b>	91.0	96.7	97.9	74.6	43.7	58.3	64.2	25.9	21.7	31.8	37.1	7.0	9.4	18.9	25.1	9.4	32.3	49.1	56.6
Market+ <b>All</b>	90.4	96.5	97.8	73.5	<b>46.3</b>	<b>61.2</b>	<b>66.8</b>	<b>26.7</b>	<b>24.4</b>	<b>35.7</b>	<b>41.0</b>	<b>7.6</b>	<b>10.0</b>	<b>20.1</b>	<b>26.0</b>	<b>9.9</b>	33.2	<b>48.1</b>	<b>58.2</b>
Duke	57.0	73.9	80.2	30.1	<b>83.5</b>	<b>91.8</b>	<b>94.3</b>	<b>70.0</b>	24.2	34.9	40.3	8.1	8.4	18.2	25.1	8.6	28.2	46.8	57.6
Duke+ <b>H</b>	62.5	78.4	83.6	32.2	82.0	91.2	94.0	68.2	26.3	37.3	42.7	8.6	8.6	17.8	22.9	8.3	30.7	48.7	57.0
Duke+ <b>S</b>	60.3	76.8	82.4	31.8	82.3	91.2	94.2	68.7	26.5	37.6	42.7	8.9	8.8	18.8	25.6	9.0	29.4	46.2	55.1
Duke+ <b>L</b>	59.6	75.2	80.9	31.1	82.4	91.4	94.1	68.5	27.1	38.2	43.5	9.2	10.6	20.6	26.6	10.4	34.5	53.2	59.5
Duke+ <b>C</b>	59.4	74.3	81.1	30.7	83.4	91.6	94.1	69.0	29.8	41.7	47.3	10.1	10.1	20.0	26.0	10.1	33.5	52.2	62.7
Duke+ <b>All</b>	<b>66.1</b>	<b>81.6</b>	<b>86.3</b>	<b>35.5</b>	81.5	90.8	93.1	65.9	<b>35.5</b>	<b>48.2</b>	<b>53.7</b>	<b>12.2</b>	<b>10.7</b>	<b>21.9</b>	<b>27.5</b>	<b>10.5</b>	<b>35.4</b>	<b>54.1</b>	<b>62.3</b>



Figure 7: Visual comparison between UML and SPGAN on (top) DukeMTMC-reID and (bottom) Market-1501.

Seed	Method	Duke			
		R1	R5	R10	mAP
Market	UML	46.3	61.2	66.8	26.7
	UML+SPGAN	<b>46.9</b>	<b>62.2</b>	<b>67.7</b>	<b>27.0</b>
Seed	Method	Market			
		R1	R5	R10	mAP
Duke	UML	<b>66.1</b>	<b>81.6</b>	<b>86.3</b>	<b>35.5</b>
	UML+SPGAN	65.5	81.2	85.8	35.2

Table 6: SPGAN on top of UML.

ment across heterogeneous domains. This is consistent with the observations made in Tables 3 and 4.

**Comparison to state-of-the-art image synthesis.** As an image generation method, we specially compared our UML with the state-of-the-art image synthesis model SPGAN (Deng et al. 2018). We did not select HHL (Zhong et al. 2018) since it is a hybrid of image synthesis and cross-domain feature learning. We have already compared the quantitative results in Table 3, and showed that SPGAN is inferior. This is intuitively reasonable as observed from the visual comparison of them in Fig. 7. Specifically, UML generates much more diverse and richer images than SPGAN in a computationally more efficient and domain generic man-

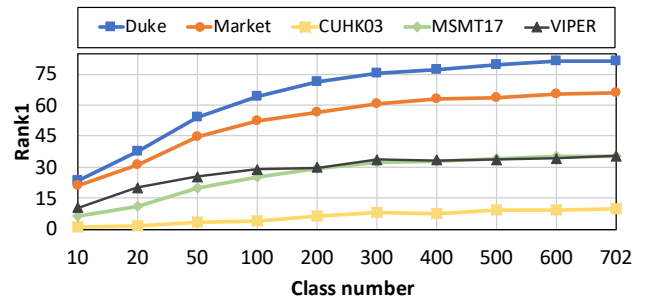


Figure 8: Effect of seed identity class number. Seed domain: DukeMTMC-reID.

ner. On the contrary, SPGAN requires computationally expensive domain-specific model training along with tedious hyper-parameter tuning. By only altering the colour and contrast properties, UML can well preserve the person identity class information without the need for designing identity preserving loss function. The colour of clothing and/or associations may clearly changes w.r.t. the original seed images, but all other identity information including person physical and biometric characteristics remain. This is partly against the conventional understanding that clothing colour plays



the dominant role in person re-id therefore their variation of the same person identity class may hurt the model generalisation (Gong et al. 2014). Our investigation and finding uniquely challenge this classical wisdom and validate the importance of otherwise appearance information to person re-id. This inspires future novel ideas especially for image synthesis modelling. Functionally, SPGAN images can be considered as part of UML images. To demonstrate this, we tested the complementary effect of SPGAN on top of UML. The results in Table 6 show that very limited effect can be resulted from adding SPGAN images to the training set. This also justifies the superior performance of UML since acquisition of large scale training data is one of the key elements for ensuring model generalisation capability in deep learning.

**Seed identity class number.** We tested the effect of seed person identity class number on the model performance. We used DukeMTMC-reID as the seed training set and varied the training class number between 100 and 702. Figure 8 shows that more seed classes generally lead to better performance as expected. Surprisingly, our method is able to perform well using as few as 100 person classes ( $\frac{1}{7}$  of the standard training size). This validates the efficacy of our model in case of limited seed training data.

## Conclusion

In this work we presented a *Universal Model Learning* (UML) for domain-generic universal person re-id in a “train once, run everywhere” pattern. This differs from all the existing state-of-the-art supervised and unsupervised learning (including domain adaptation) methods typically taking a “train once, run once” pattern, suffering from per-domain *repeated* model training as well as the corresponding various costs and limitations. Our method therefore opens up a direction taking intelligent learning algorithms closer to industrial-level applications, although the current performance achieved is still inferior to that of supervised learning counterparts. As a training image generation method, our method is readily able to integrate any off-the-shelf supervised learning algorithms without extra complexity and obstacle of hyper-parameter tuning and model optimisation as required by image synthesis methods. Due to such modelling simplicity and flexibility, the proposed method serve well as a good baseline upon which further algorithm development and innovation can be established. We have conducted extensively comparative experiments for unsupervised person re-id in the unlabelled target domain using five publicly available benchmarks, and demonstrated the performance superiority and modelling advantages of UML over the state-of-the-art alternative methods in both unsupervised model learning and unsupervised domain adaptation settings. Detailed component analyses were also provided for giving insights and deep understanding about the UML model performance superiority.

## Acknowledgements

This work was partly supported by the China Scholarship Council, Vision Semantics Limited, the Royal Society Newton Advanced Fellowship Programme (NA150459), and Innovate UK Industrial Challenge Project on Developing and Commercialising Intelligent Video Analytics Solutions for Public Safety (98111-571149).

## References

- Bak, S.; Carr, Peter; and Lalonde, J.-F. 2018. Domain adaptation through synthesis for unsupervised person re-identification. In *Proceedings of the European Conference on Computer Vision (ECCV)*, 189–205.
- Chang, X.; Hospedales, T. M.; and Xiang, T. 2018. Multi-level factorisation net for person re-identification. In *CVPR*.
- Chen, Y.-C.; Zhu, X.; Zheng, W.-S.; and Lai, J.-H. 2017. Person re-identification by camera correlation aware feature augmentation. *IEEE TPAMI*.
- Chen, Y.; Zhu, X.; and Gong, S. 2017. Person re-identification by deep learning multi-scale representations. In *ICCV Workshop*.
- Chen, Y.; Zhu, X.; and Gong, S. 2018. Deep association learning for unsupervised video person re-identification. In *BMVC*.
- Cheng, D. S.; Cristani, M.; Stoppa, M.; Bazzani, L.; and Murino, V. 2011. Custom pictorial structures for re-identification. In *BMVC*.
- Deng, W.; Zheng, L.; Kang, G.; Yang, Y.; Ye, Q.; and Jiao, J. 2018. Image-image domain adaptation with preserved self-similarity and domain-dissimilarity for person reidentification. In *CVPR*.
- Fan, H.; Zheng, L.; and Yang, Y. 2017. Unsupervised person re-identification: clustering and fine-tuning. *arXiv*.
- Farenzena, M.; Bazzani, L.; Perina, A.; Murino, V.; and Cristani, M. 2010. Person re-identification by symmetry-driven accumulation of local features. In *CVPR*.
- Gholami, B.; Sahu, P.; Rudovic, O.; Bousmalis, K.; and Pavlovic, V. 2018. Unsupervised multi-target domain adaptation: An information theoretic approach. *arXiv preprint arXiv:1810.11547*.
- Gong, S.; Cristani, M.; Yan, S.; and Loy, C. C. 2014. *Person re-identification*. Springer.
- Goodfellow, I.; Pouget-Abadie, J.; Mirza, M.; Xu, B.; Warde-Farley, D.; Ozair, S.; Courville, A.; and Bengio, Y. 2014. Generative adversarial nets. In *Advances in neural information processing systems*, 2672–2680.
- Gray, D., and Tao, H. 2008. Viewpoint invariant pedestrian recognition with an ensemble of localized features. In *European conference on computer vision*, 262–275. Springer.
- Haerberli, P., and Voorhies, D. 1994. Image processing by linear interpolation and extrapolation. *IRIS Universe Magazine* 28:8–9.
- He, K.; Zhang, X.; Ren, S.; and Sun, J. 2016. Deep residual learning for image recognition. In *CVPR*.
- Kodirov, Elyor; Xiang, T.; and Gong, S. 2015. Dictionary learning with iterative laplacian regularisation for unsupervised person re-identification. In *BMVC*, volume 3, 8.
- Krizhevsky, A.; Sutskever, I.; and Hinton, G. E. 2012. Imagenet classification with deep convolutional neural networks. In *Advances in neural information processing systems*, 1097–1105.
- Li, W.; Zhao, R.; Xiao, T.; and Wang, X. 2014. Deepreid: Deep filter pairing neural network for person re-identification. In *CVPR*.
- Li; Minxian; Zhu, X.; and Gong, S. 2018. Unsupervised person re-identification by deep learning tracklet association. In *Proceedings*

- of the *European Conference on Computer Vision (ECCV)*, 737–753.
- Li, W.; Zhu, X.; and Gong, S. 2017. Person re-identification by deep joint learning of multi-loss classification.
- Li, W.; Zhu, X.; and Gong, S. 2018. Harmonious attention network for person re-identification. In *CVPR*.
- Liao, S.; Hu, Y.; Zhu, X.; and Li, S. Z. 2015. Person re-identification by local maximal occurrence representation and metric learning. In *CVPR*.
- Lin, S.; Li, H.; Li, C.-T.; and Kot, A. C. 2018. Multi-task mid-level feature alignment network for unsupervised cross-dataset person re-identification. *arXiv*.
- Lin, Y.; Dong, X.; Zheng, L.; Yan, Y.; and Yang, Y. 2019. A bottom-up clustering approach to unsupervised person re-identification. In *AAAI Conference on Artificial Intelligence*.
- Lisanti, G.; Masi, I.; Bagdanov, A. D.; and Del Bimbo, A. Person re-identification by iterative re-weighted sparse ranking. *IEEE transactions on pattern analysis and machine intelligence*.
- Munsell color system. [https://en.wikipedia.org/wiki/Munsell\\_color\\_system](https://en.wikipedia.org/wiki/Munsell_color_system).
- Munsell, A. H. 1919. *A color notation*. Munsell color company.
- Paszke, A.; Gross, S.; Chintala, S.; Chanan, G.; Yang, E.; DeVito, Z.; Lin, Z.; Desmaison, A.; Antiga, L.; and Lerer, A. 2017. Automatic differentiation in pytorch.
- Peng, P.; Xiang, T.; Wang, Y.; Pontil, M.; Gong, S.; Huang, T.; and Tian, Y. 2016. Unsupervised cross-dataset transfer learning for person re-identification. In *CVPR*.
- Qian, X.; Fu, Y.; Xiang, T.; Wang, W.; Qiu, J.; Wu, Y.; Jiang, Y.-G.; and Xue, X. 2018. Pose-normalized image generation for person re-identification. In *Proceedings of the European Conference on Computer Vision (ECCV)*, 650–667.
- Russakovsky, O.; Deng, J.; Su, H.; Krause, J.; Satheesh, S.; Ma, S.; Huang, Z.; Karpathy, A.; Khosla, A.; Bernstein, M.; et al. 2015. Imagenet large scale visual recognition challenge. *International journal of computer vision* 115(3):211–252.
- Shen, Y.; Li, H.; Yi, S.; Chen, D.; and Wang, X. 2018. Person re-identification with deep similarity-guided graph neural network. In *The European Conference on Computer Vision (ECCV)*.
- Song, C.; Huang, Y.; Ouyang, W.; and Wang, L. 2018. Mask-guided contrastive attention model for person re-identification. In *CVPR*.
- Sun, Y.; Zheng, L.; Yang, Y.; Tian, Q.; and Wang, S. 2018. Beyond part models: Person retrieval with refined part pooling (and a strong convolutional baseline). In *ECCV*.
- Wang, G.; Yuan, Y.; Chen, X.; Li, J.; and Zhou, X. Learning discriminative features with multiple granularities for person re-identification. In *2018 ACM Multimedia Conference on Multimedia Conference*.
- Wang, T.; Gong, S.; Zhu, X.; and Wang, S. 2014. Person re-identification by video ranking. In *ECCV*.
- Wang, C.; Zhang, Q.; Huang, C.; Liu, W.; and Wang, X. 2018a. Mancs: A multi-task attentional network with curriculum sampling for person re-identification. In *ECCV*.
- Wang, J.; Zhu, X.; Gong, S.; and Li, W. 2018b. Transferable joint attribute-identity deep learning for unsupervised person re-identification. *arXiv*.
- Wei, L.; Zhang, S.; Gao, W.; and Tian, Q. 2017. Person transfer gan to bridge domain gap for person re-identification. In *CVPR*.
- Wei, L.; Zhang, S.; Gao, W.; and Tian, Q. 2018. Person transfer gan to bridge domain gap for person re-identification. In *Proceedings of the IEEE Conference on Computer Vision and Pattern Recognition*, 79–88.
- Xiao, T.; Li, H.; Ouyang, W.; and Wang, X. 2016. Learning deep feature representations with domain guided dropout for person re-identification. In *CVPR*.
- Xu, J.; Zhao, R.; Zhu, F.; Wang, H.; and Ouyang, W. 2018. Attention-aware compositional network for person re-identification. *arXiv*.
- Yu, R.; Dou, Z.; Bai, S.; Zhang, Z.; Xu, Y.; and Bai, X. 2018. Hardware-aware point-to-set deep metric for person re-identification. In *The European Conference on Computer Vision (ECCV)*.
- Yu, H.-X.; Wu, Ancong; and Zheng, W.-S. 2019. Unsupervised person re-identification by deep asymmetric metric embedding. *IEEE transactions on pattern analysis and machine intelligence*.
- Yu, H.; Hu, M.; and Chen, S. 2018. Multi-target unsupervised domain adaptation without exactly shared categories. *arXiv preprint arXiv:1809.00852*.
- Yu, H.-X.; Wu, A.; and Zheng, W.-S. 2017. Cross-view asymmetric metric learning for unsupervised person re-identification. In *ICCV*.
- Zhang, Y.; Xiang, T.; Hospedales, T. M.; and Lu, H. 2018. Deep mutual learning. *CVPR*.
- Zhao, R.; Oyang, W.; and Wang, X. 2017. Person re-identification by saliency learning. *IEEE TPAMI*.
- Zheng, L.; Shen, L.; Tian, L.; Wang, S.; Wang, J.; and Tian, Q. 2015. Scalable person re-identification: A benchmark. In *ICCV*.
- Zheng; Zhedong; Zheng, L.; and Yang, Y. 2017. Unlabeled samples generated by gan improve the person re-identification baseline in vitro. *arXiv*.
- Zhong, Z.; Zheng, L.; Li, S.; and Yang, Y. 2018. Generalizing a person retrieval model hetero- and homogeneously. In *ECCV*.